HYDRATED MINERALS ASSOCIATED WITH INTERIOR LAYERED DEPOSITS NEAR THE SOUTHERN WALL OF MELAS CHASMA, VALLES MARINERIS, MARS. Yang Liu[1], R. E. Arvidson[1], R. Li[2], and W. Wang[2], [1]Department of Earth and Planetary Sciences and McDonnell Center for Space Sciences, Washington University, Campus Box 1169, Saint Louis, MO 63130, USA (liuyang@levee.wustl.edu), [2]Mapping and GIS Laboratory, The Ohio State University Dept. of Civil & Env. Eng. & Geodetic Science, Columbus, OH 43210.

Introduction: Melas Chasma is the widest segment of the Valles Marineris on Mars and is located in the center of this canyon system. It contains extensive and highly organized valley networks that have been interpreted to have been fed by precipitation since the heads of valleys are scattered at different elevations [1,2]. Many complex sedimentary landforms such as interior layered deposits (ILDs) have been observed in Melas Chasma whose origin is one of the key issues for understanding the evolution of the canyon [e.g., 3-5]. Hydrated sulfates have been identified in Melas Chasma by both OMEGA and CRISM at different locations in Melas Chasma, and most of the identifications are associated with layered deposits [e.g., 6,7].

In this study, we identified a sequence of interior layered deposits over a portion of the southern wall and nearby floor of Melas Chasma as inferred from MRO CRISM full resolution targeted mode hyperspectral image data (FRT00013F5B) centered at 10.22 S, 74.46 W (Fig 1). Polyhydrated sulfates, monohydrated sulfates, and jarosite were identified in the ILDs and extended areas. Superposition relationships and stratigraphic orders were defined with the help of HiRISE images.

Data Sets: The Compact Reconnaissance Imaging Spectrometer for Mars (CRISM) on board Mars Reconnaissance Orbiter (MRO) is a hyperspectral imager which has been acquiring data since November 2006 [8]. CRISM has 544 wavelength channels covering 0.36-3.92 μm and has a spatial resolution of 18-36 m per pixel in targeted mode. The High Resolution Imaging Science Experiment (HiRISE) instrument is co-aligned with CRISM and provides high-resolution (0.25 m/pixel) images [9] that complement the CRISM spectral imaging observations.

Spectral Results: CRISM I/F data were atmospherically corrected using the standard "volcano scan" method [10]. The spectra shown are the ratios between hydrated mineral exposures and spectrally bland areas in the same scene with 5x5 pixel sizes. Monohydrated sulfates, polyhydrated sulfates, and jarosite were identified using CRISM spectra. Hydrated sulfates have an absorption feature at 2.4 μm that is due to overtones of $(SO_4)^{2-}$ stretching fundamentals ($3\nu_3$) associated with H_2O or OH [11]. Specifically, monohydrated sulfates were identified by absorption features at 1.6 and ~2.1 μm, polyhydated sulfates were identified based on the absorption features near 1.4 and 1.9 μm, and jarosite was identified by absorption features at ~1.46, 1.85, and 2.265 μm (Fig 1).

Stratigraphic Relationships: A HiRISE DEM generated at The Ohio State Univerity [12], together with CRISM spectral parameter maps [13], were used to define stratigraphic relationships associated with hydrated materials (Figs 2 and 3). The ILDs have been eroded into a bowl shape bounded by a capping, bench-like unit with a jarosite signature (Fig 3). Both jarosite and polyhydrated sulfates were identified immediately downslope of the cap unit. The area with

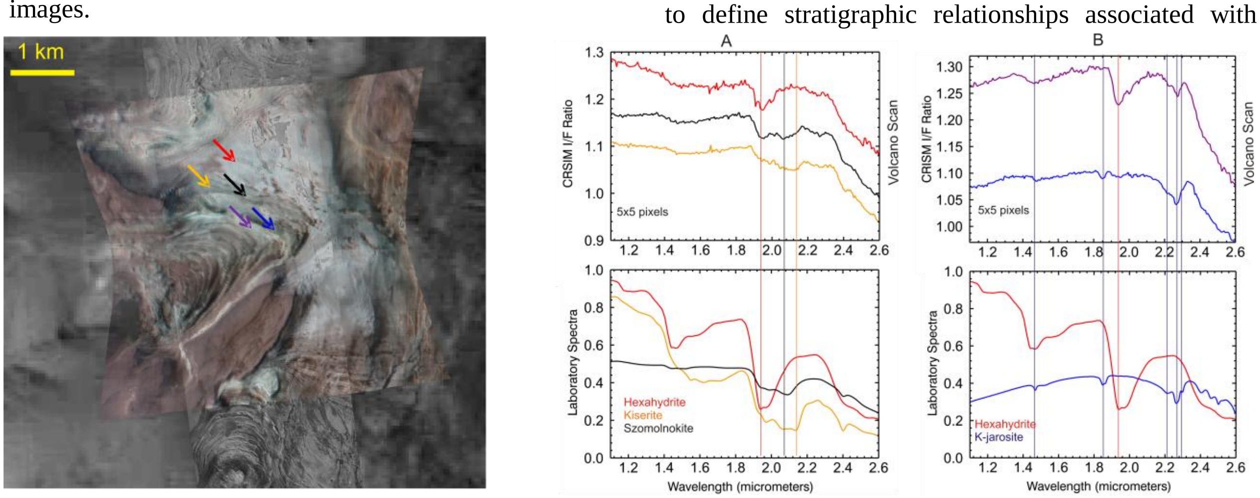

Figure 1 (left) CRISM FRT00013F5B I/F false color composite image over HRSC and HiRSE images shows light-toned materials in the ILDs. The arrows indicate the areas where the spectra were collected. (right) Comparison between inferred CRISM hydrated sulfate and laboratory spectra.

relatively pure jarosite is darker and smoother, while the area with both jarosite and polyhydrated suflates is brighter and exhibits a fractured appearance. Within the bowl, interbedded monohydrated and polyhydrated sulfate-bearing layers are exposed (Fig 2). Roach et al. found similar alternating mono- and poly-hydrated sulfate layers in the East Candor ILDs, and has proposed several models to explain the formation mechanism [14]. ILDs are also exposed to the northeast dipping away from the cap unit. A lower bench (Fig 3) is exposed with a monohydrated sulfate signature. Below the second bench is an areally extensive polyhydrated sulfate-bearing unit.

Conclusions and Future Work: Monohydrated sulfate, polyhydrated sulfate, and jarosite were identified in the ILDs near the southern wall of Melas Chasma with distinct stratigraphic relationships. Interbedded mono- and poly-hydrated sulfate bearing layers were observed. In the future, DISORT radiative transfer models [15] will be used to retrieve surface single scattering albedos including modeling local slope effects on lighting and viewing angles. Many exposures of light-toned materials associated with ILDs are visible in the HiRISE data, and future along-track oversampled CRISM data will allow us to resolve more layers. Finally analyses of the apparently cyclical changing aqueous conditions inferred from the mineral associations will be conducted.

Acknowledgement: We are grateful to CRISM and HiRISE science teams for all their dedication. Thanks to S. L. Murchie for his thoughtful comments.

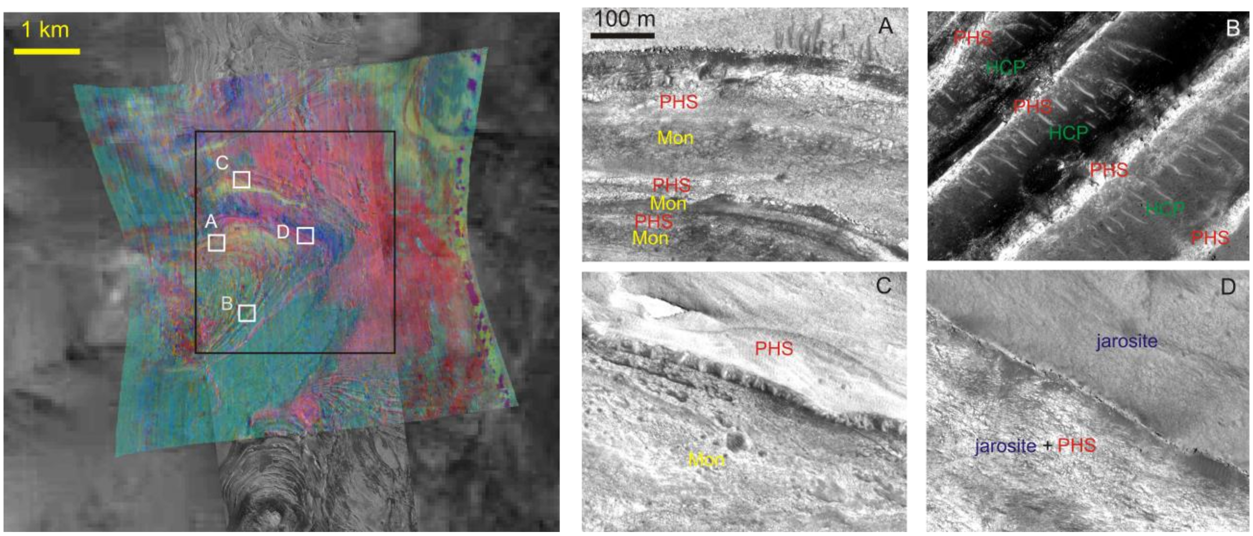

Figure 2 (left) CRISM parameter map over HRSC and HiRISE images (red, SINDEX; green 2100BD; blue, 2265BD, which indicate polyhydrated sulfate, monohydrated sulfate, and jarosite, respectively). (Right) HiRISE subset images show types of stratigraphy of hydrated minerals. (Note: PHS = polyhydrated sulfates, Mon = monohydrated sulfates, HCP = high-calcium pyroxene)

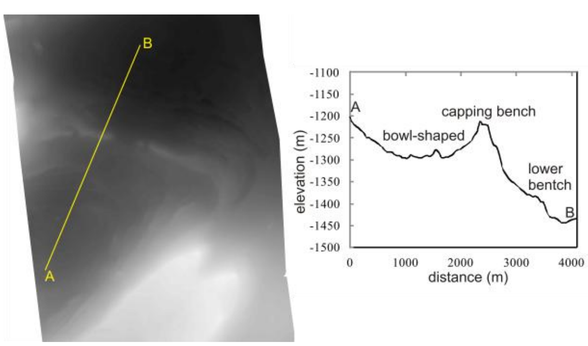

Figure 3 (left) Transect in yellow over HiRISE DEM (from black box in Fig 2 left image) ending at B. (right) Inferred topographic profile showing the change of the elevation from A to B.

References: [1] Mangold et al. (2004) *Science*, *305*, 78-81. [2] Quantin C. et al. (2005) *JGR*, *110*, E12S19. [3] Lucchitta B. K. et al. (1994) *JGR*, *99*, 3783-3798. [4] Nedell S. et al. (1987), *Icarus*, *70*, 409-441. [5] Chapman M. G. and K. L. Tanaka (2001), *JGR*, *106*, 10087-10100. [6] Gendrin A. et al., (2005) *Science*, *307*, 1587-1591. [7] Weitz et al. (2009) *LPSC XL*, Abstract #1874. [8] Murchie S.L. et al. (2007) *JGR 112*, E05S03. [9] McEwen A. et al. (2007) *JGR*, *109*, E06005. [10] Mustard et al. (2008), *Nature*, *454*, 305-309. [11] Cloutis E.A. et al. (2006) *Icarus*, *184*, 121-157. [12] Li R. et al. (2011) *IEEE TGRS*, *49*, 2558-2572. [13] Pelky S.M. et al (2009) *JGR*, *112*, E08S14 [14] Roach L.H. et al. (2009) *JGR 114*, E00D02. [15] Stamnes K. et al. (1998) *Appl. Opt.*, 27.